The Cytochrome P-450$_{cam}$ Binding Surface As Defined by Site-Directed Mutagenesis and Electrostatic Modeling†

Patrick S. Stayton and Stephen G. Sligar*
Departments of Biochemistry and Chemistry, University of Illinois, Urbana, Illinois 61801
Received December 6, 1989; Revised Manuscript Received April 19, 1990

ABSTRACT: Cytochrome P-450$_{cam}$ cationic surface charges at Lys 344, Arg 72, and Lys 392 have been altered by site-directed mutagenesis techniques. The residues at Lys 344 and Arg 72 were previously suggested as salt bridge contacts in the cytochrome b_5–cytochrome P-450$_{cam}$ association complex and implicated in the physiological putidaredoxin–cytochrome P-450$_{cam}$ complex [Stayton, P. S., Poulos, T. L., & Sligar, S. G. (1989) *Biochemistry 28*, 8201–8205]. Mutations to neutralize the basic charge at Arg 72 (R72Q) and to both neutralize and reverse the charge at Lys 344 (K344Q, K344E) resulted in alteration of NADH oxidation rates in the reconstituted physiological electron-transfer system, which is rate limited by putidaredoxin–cytochrome P-450$_{cam}$ electron transfer. The steady-state V_{max} values were apparently unperturbed, suggesting that the observed rate differences were largely attributable to K_m effects. The K_m values observed for the K344Q (24 μM) and K344E (32 μM) mutants are in the direction expected for neutralization and reversal of a salt bridge charge interaction. A control mutation at a basic surface charge located away from the proposed site of interaction, Lys 392 (K392Q), resulted in overall activities quantitated by NADH oxidation rates that are similar to that of wild-type cytochrome P-450$_{cam}$. Calculation of the cytochrome P-450$_{cam}$ electrostatic field revealed a patch of positive potential at the modeled cytochrome b_5 interaction site lying directly above the nearest proximal approach to the buried heme prosthetic group. These results provide experimental and theoretical evidence for the modeled cytochrome P-450$_{cam}$ binding site implicated in both cytochrome b_5 and putidaredoxin association. These results also provide an interesting framework for consideration of how well eukaryotic sequences and functional studies correlate with the cytochrome P-450$_{cam}$ structural model.

The cytochromes P-450 catalyze a complex array of difficult chemical transformations that require a correspondingly complex set of interprotein relationships. Protein–protein interactions provide the means for electron transfer, the process of which is utilized as the rate-limiting step in the reaction cycle (Pederson et al., 1977; Hintz & Peterson, 1981; Hintz et al., 1982; Brewer & Peterson, 1988), and also in some cases provide a necessary effector function that couples the flow of reducing equivalents to successful substrate turnover (Sligar et al., 1974; Lipscomb et al., 1976; Tsubaki et al., 1988). In addition, certain eukaryotic P-450 isozymes are functionally separable in their requirement of different protein partners during the catalytic cycle (Morgan & Coon, 1984; Black & Coon, 1987). These interactions are well understood in chemical and kinetic terms but have been poorly characterized at the level of detailed molecular structure.

Cytochrome P-450$_{cam}$ has served as the prototypal model for this family of enzymes due to its solubility and availability in large quantities. It serves as a direct model of structure and function relationships as it represents the only cytochrome P-450 for which a high-resolution crystal structure has been determined (Poulos et al., 1985, 1986, 1987). To the extent that the bacterial cytochrome P-450 model may be hypothetically extended to eukaryotic cytochrome P-450 structures, it is of general interest to characterize its protein interaction surface in molecular detail.

Electrostatic forces have been shown to play an important role in both eukaryotic and bacterial cytochrome P-450$_{cam}$ protein–protein interactions (Bernhardt et al., 1984; Nadler & Strobel, 1988; Stayton et al., 1988; Lambeth et al., 1984; Hintz & Peterson, 1981; Lambeth & Kriengsiri, 1985). A specific cytochrome P-450$_{cam}$ binding site that includes electrostatic salt bridge contacts has been proposed for the association of cytochrome b_5 and the physiological protein reductant putidaredoxin (Stayton et al., 1988, 1989). The contribution of modeled cytochrome P-450$_{cam}$ salt bridge contacts to physiological complex formation can be tested with site-directed surface charge mutants that remove the basic side chains of P-450. As reported in this paper, these mutants provide the first experimental evidence in favor of a specific binding site from the cytochrome P-450$_{cam}$ side of the diprotein complex.

The availability of a refined crystal structure also makes it possible to calculate an electrostatic potential field for cytochrome P-450$_{cam}$. The resultant view of the electrostatic surface agrees well with our previous modeling studies and gives an easily visualized rationale for the surface charge mutant effects on putidaredoxin association. The mapping of the cytochrome P-450$_{cam}$ electrostatic surface is also used in comparing both experimental and theoretical work suggesting the existence of conserved binding surfaces throughout the cytochrome P-450 family (Nelson & Strobel, 1988; Tuls et al., 1989; Tsubaki et al., 1989).

Materials and Methods

Site-Directed Mutagenesis of Cytochrome P-450$_{cam}$. Single-stranded mutagenesis techniques (Taylor et al., 1985) utilizing a commercially available kit (Amersham) were used to produce the desired mutants. The camA *Pst*I/*Hin*dIII fragment (Unger et al., 1986) was subcloned into M13mp10, and previously described slight modifications (Atkins & Sligar, 1988) of the commercial protocol followed. Correct generation

† This research was supported by National Institutes of Health Grants GM 32620 and GM 31756.
* To whom correspondence should be addressed.

0006-2960/90/0429-7381$02.50/0

of the single mutations was confirmed by DNA sequencing. Lys 344 was altered to Gln 344 and Glu 344 with a mixed mutagenic primer, Arg 72 similarly mutated to Gln 72 and Glu 72, and Lys 392 changed to Gln 392. The mutated *PstI*/*KpnI* fragments were subsequently cloned back into pUC19 for expression in *Escherichia coli*.

Expression and Purification of Mutant Proteins. The mutants at position 344 and 392 were overexpressed at normal wild-type levels (Unger et al., 1986) in *E. coli*. R72Q[1] was expressed at reduced levels while R72E was expressed at extremely low levels and proved to be unstable during the purification process. The four mutants K344Q, K344E, K392Q, and R72Q were purified from *E. coli* strain TG-1 (Amersham) by slight modifications of the protocol used for purification from the native *Pseudomonas* system (Gunsalus & Wagner, 1978). These modifications were elimination of the ammonium sulfate salt cut and substitution of ACA-44 gel filtration resin (LKB) for the molecular sieving step. Putidaredoxin and putidaredoxin reductase were purified as previously described (Gunsalus & Wagner, 1976).

NADH Oxidation Assays. NADH oxidation was monitored at 340 nm on an HP8450 UV–visible spectrophotometer, temperature controlled at 22 °C. Assays utilized 425 μM *d*-camphor, 200 mM KCl, 0.8 μM cytochrome P-450$_{cam}$, 2 μM putidaredoxin reductase, 150 μM NADH, and 50 mM Tris, pH 7.4, and the putidaredoxin concentration was varied. The camphor-dependent NADH consumption was linear, and rates were calculated with an extinction coefficient of 6.22 mM^{-1} cm^{-1} for NADH.

Electrostatic Potential Calculations. The electrostatic potential field was calculated with a commercially available (Biosym Technologies, San Diego, CA) version of DELPHI, originally developed by Honig and co-workers (Gilson & Honig, 1988). This algorithm uses a two-continuum treatment of the dielectric properties of the system and uses a finite difference solution of the Poisson–Boltzmann equation to solve for the electrostatic potential. A discrete charge library was utilized to define the contributing charged atoms whose location was specified by the cytochrome P-450$_{cam}$ crystal structure (Poulos et al., 1987). Specifically, the following charge assignments were utilized. The lysine side-chain nitrogen was assigned a charge of +1.0, the guanidinium nitrogens of arginine +0.5 each, the carboxylate oxygens of glutamate and aspartate −0.5 each, the imidazole nitrogens of histidine +0.25 each, and the axial thiolate sulfur −1.0. In addition, the C-terminus was assigned a −1.0 charge, the heme prosthetic group was given a charge of +1.0 at the iron, and the heme propionates were assigned −0.5 at the carboxylate oxygens. The interior dielectric was assigned a value of 2 while the exterior was assigned a value of 80, with the ionic strength specified to 140 mM. The mutant electrostatic fields were calculated in identical fashion, with use of a coordinate file differing only in the replacement of the single surface amino acid with glutamine or glutamate.

RESULTS

Cytochrome P-450$_{cam}$ Charge Mutants. Surface charge mutants were generated at residue Lys 344, where the positive charge was both reversed to a negative charge by mutation to glutamate and neutralized by mutation to glutamine, and at residues Arg 72 and Lys 392, where the positive charges were neutralized via mutation to glutamine. These first two residues have been implicated in modeling studies of cytochrome b_5–cytochrome P-450$_{cam}$ association (Stayton et al., 1989) and hypothetically extended to the physiological putidaredoxin–cytochrome P-450$_{cam}$ complex in binding competition studies (Stayton et al., 1989). In order to ascertain the role of these residues in macromolecular recognition, the effects of mutations at these positions on putidaredoxin association were estimated with kinetic measurements utilizing a tightly coupled NADH oxidation assay which is known to be rate limited by electron transfer from putidaredoxin to cytochrome P-450$_{cam}$ (Pederson et al., 1977; Brewer & Peterson, 1988). These can thus be used to estimate the relative putidaredoxin–cytochrome P-450$_{cam}$ affinity by studying the rates as a function of putidaredoxin concentration where observed rates would be expected to be particularly sensitive at low ratios of putidaredoxin to cytochrome P-450$_{cam}$. In these experiments the mutants were always measured side by side with wild-type cytochrome P-450$_{cam}$ and the results normalized to a standard wild-type rate. In addition, the concentrations of mutant and wild-type cytochromes P-450$_{cam}$ were kept identical in all the assays. The mutations at positions Lys 344 and Arg 72 displayed wild-type, high-spin ($S = {}^5/_2$), camphor-bound ferric EPR spectra (data not shown), suggesting that the active site electronic structure was unperturbed by the surface charge mutations.

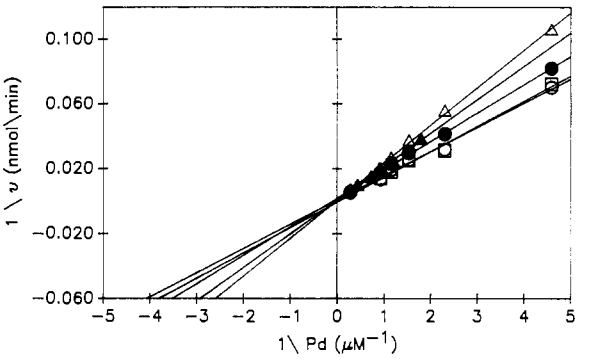

FIGURE 1: Double-reciprocal plots of NADH consumption rate analyses for the cytochrome P-450$_{cam}$ surface charge mutants as a function of putidaredoxin concentration. The symbols represent the following: (○) wild type; (□) K392Q; (●) K344Q; (△) K344E; (▲) R72Q.

The resultant rates were analyzed with standard double-reciprocal plots. The results of these determinations with K344Q, K344E, R72Q, and K392Q are shown in Figure 1. The mutants at positions 344 and 72 displayed altered rate profiles in a direction suggesting an altered K_m with nearly identical V_{max} values under saturating putidaredoxin–cytochrome P-450$_{cam}$ ratios. This suggestion is further supported by independent and direct measurements of the first electron-transfer rate between reduced putidaredoxin and oxidized cytochrome P-450$_{cam}$ at saturating protein concentrations (data not shown). The mutant electron-transfer rates were identical with that observed with the native wild-type protein. While potential second electron-transfer rate differences cannot be ruled out in the NADH oxidation rate assays, the convergence at the y intercept supports the simplifying assumption that the altered rate profiles result largely from perturbation of the putidaredoxin–cytochrome P-450$_{cam}$ association reaction rather than electron-transfer rate differences. The K_m differences relative to wild type range from 20% to 60% (wild type = 20 μM; K344Q = 24 μM; K344E = 32 μM; R72Q = 28 μM;

[1] Abbreviations: R72Q, mutant cytochrome P-450$_{cam}$ where Arg 72 has been changed to Gln; R72E, mutant cytochrome P-450$_{cam}$ where Arg 72 has been changed to Glu; K344Q, mutant cytochrome P-450$_{cam}$ where Lys 344 has been changed to Gln; K344E, mutant cytochrome P-450$_{cam}$ where Lys 344 has been changed to Glu; K392Q, mutant cytochrome P-450$_{cam}$ where Lys 392 has been changed to Gln; NADH, reduced nicotinamide adenine dinucleotide.

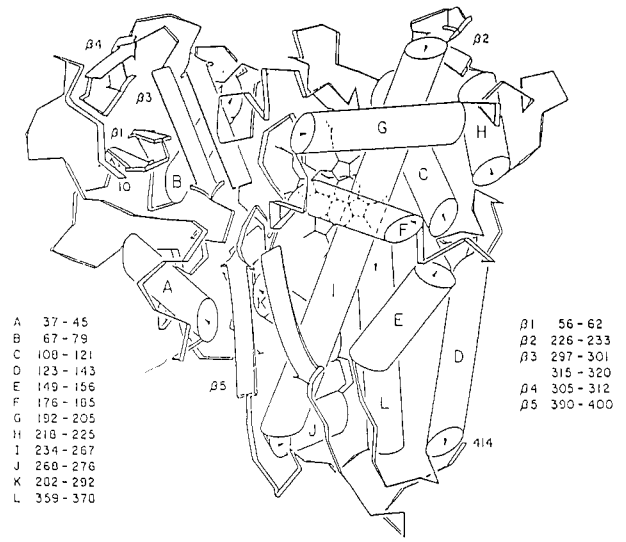

FIGURE 2: Schematic of cytochrome P-450$_{cam}$ representing the standard view. α-Helical and β-sheet segments are noted. The distal surface of the triangular wedge faces the viewer, while the proximal surface including the modeled putidaredoxin interaction domain and the axial cysteine lies on the opposite face.

K392Q = 19 μM) in calculations made with the assumption that V_{max} is unaltered. These differences are fairly small as is expected for single charge changes in an association reaction where both electrostatic and hydrophobic interactions contribute to the binding free energy. The results observed with the Lys 344 mutants follow the expected trend of greater perturbation upon reversal of the cationic surface charge to glutamate compared to neutralization with glutamine.

Cytochrome P-450$_{cam}$ Electrostatic Field. The electrostatic potential field was calculated for cytochrome P-450$_{cam}$ by use of a discrete charge library and the linearized, finite-difference Poisson–Boltzmann method. The DELPHI software package allows the use of partial charge libraries such as AMBER or CHARMM, which explicitly consider atomic charges. This type of calculation is able to account for effects such as the macroscopic dipoles resulting from α-helical segments, although better reproduction of electrostatic conditions in the interior of proteins requires a complete self-consistent field calculation rather than a two-continuum approximation of bulk dielectric constants (Warshel, 1984). Surface fields can usually be reasonably approximated by consideration of the discrete charges arising from ionizable amino acid side chains which greatly outnumber the major helical stretches. In addition, the helix termini would have to lie very near the surface to contribute significantly since their effect dissipates in a sharply distance-dependent manner. Cytochrome P-450$_{cam}$ contains several helical segments that are generally localized in half of the molecule, and thus, it would be interesting to do a rigorous partial charge library based calculation to test for the effect of these secondary structure elements. The present report, however, only considers the ionizable amino acid side chains.

The general features of the cytochrome P-450$_{cam}$ electrostatic surface can be seen in Figure 3. The following description will be made in terms of what has been called the "standard view" of the cytochrome P-450$_{cam}$ molecule (Poulos et al., 1987). This orientation places the heme group in the plane of the page with the camphor binding pocket facing the viewer, so that the molecule appears as a triangular wedge (Figure 2). The axial cysteine lies behind the page on what is termed the proximal surface. The blue contours in Figure 3 represent anionic potential at an energy level of 3 kT while the yellow contours denote the cationic analogue. The negative field dominates the cytochrome P-450$_{cam}$ surface with a particularly extensive localization of anionic charge on the distal surface. A lobe of negative potential is concentrated on the α-helical-rich domain of the cytochrome P-450$_{cam}$ structure. The only patches of cationic potential lie on the proximal surface directly above the axial cysteine and along the side of the triangular wedge. The largest continuous patch of cationic potential lies directly above the proximal cysteine ligand and is generated by basic residues including Arg 72, Lys 344, Arg 364, and Arg 112. This patch is roughly circular with a diameter of approximately 20 Å. The mutant cationic fields at this proximal patch are reduced as would be expected for the removal of a basic side chain (Figure 3b–d) with a particularly notable effect for the K344E mutant. The K392Q mutation does not alter the calculated field at the distant proximal cationic patch. At low ionic strength the negative surface at 3 kT is extended into solution approximately 7 Å while the positive surface is less extended. The high ionic strength surface is reduced as expected due to shielding of charge by mobile ions.

DISCUSSION

Electrostatic contributions to protein–protein association processes have been observed in a number of electron-transfer complexes composed of heme protein redox partners (Salemme, 1976; Ng et al., 1977; Ferguson-Miller et al., 1978; Geren & Millett, 1981; Hackett & Strittmatter, 1984; Poulos & Finzel, 1987; Poulos & Mauk, 1983). The apparent charge complementarity of these donor and acceptor surfaces has been used to model potential complex geometries (Salemme, 1976; Poulos & Finzel, 1987; Poulos & Mauk, 1983). While the observation of these charged residues near the presumed site of electron transfer is widespread, their precise function is less clear. Salt bridge formation is not expected to account for a majority of binding free energies observed with heme protein association (Rodgers et al., 1988). Rather, hydrophobic and van der Waals forces spread over the entire interaction surface are likely to account for much of this energy. Various other roles for electrostatic interactions have been proposed, including longer range steering of bimolecular trajectories (Matthew et al., 1983; Wendoloski et al., 1987; Northrup et al., 1988) and direction of prosthetic group orientation to ensure efficient electron-transfer geometry (Salemme, 1976; Hazzard et al., 1988; Wendoloski et al., 1987).

The purpose of the work reported in this paper is to define the surface domain of cytochrome P-450$_{cam}$ which interacts with its redox partner. The altered rates of NADH consumption exhibited by the surface charge mutants at Lys 344 and Arg 72 could potentially arise from perturbation of the putidaredoxin–cytochrome P-450$_{cam}$ binding free energy, which should be reflected in K_m differences, or from orientational alterations resulting in electron-transfer rate differences, which would be reflected in differences in the maximal velocity of NADH oxidation. From the results reported herein, the major effects of these mutations are on the putidaredoxin–cytochrome P-450$_{cam}$ binding equilibrium. Similarly, the orientation of the complex seems to be largely conserved, since geometry alterations might be expected to affect the maximal rates of electron transfer. The K344E mutant shows the largest y intercept deviation and may result in some perturbation of the relative orientation of the redox centers. The overall magnitude of the effects is small, consistent with single charge mutations involving electrostatic components of the binding free energy which is probably dominated by hydrophobic and van der Waals contributions.

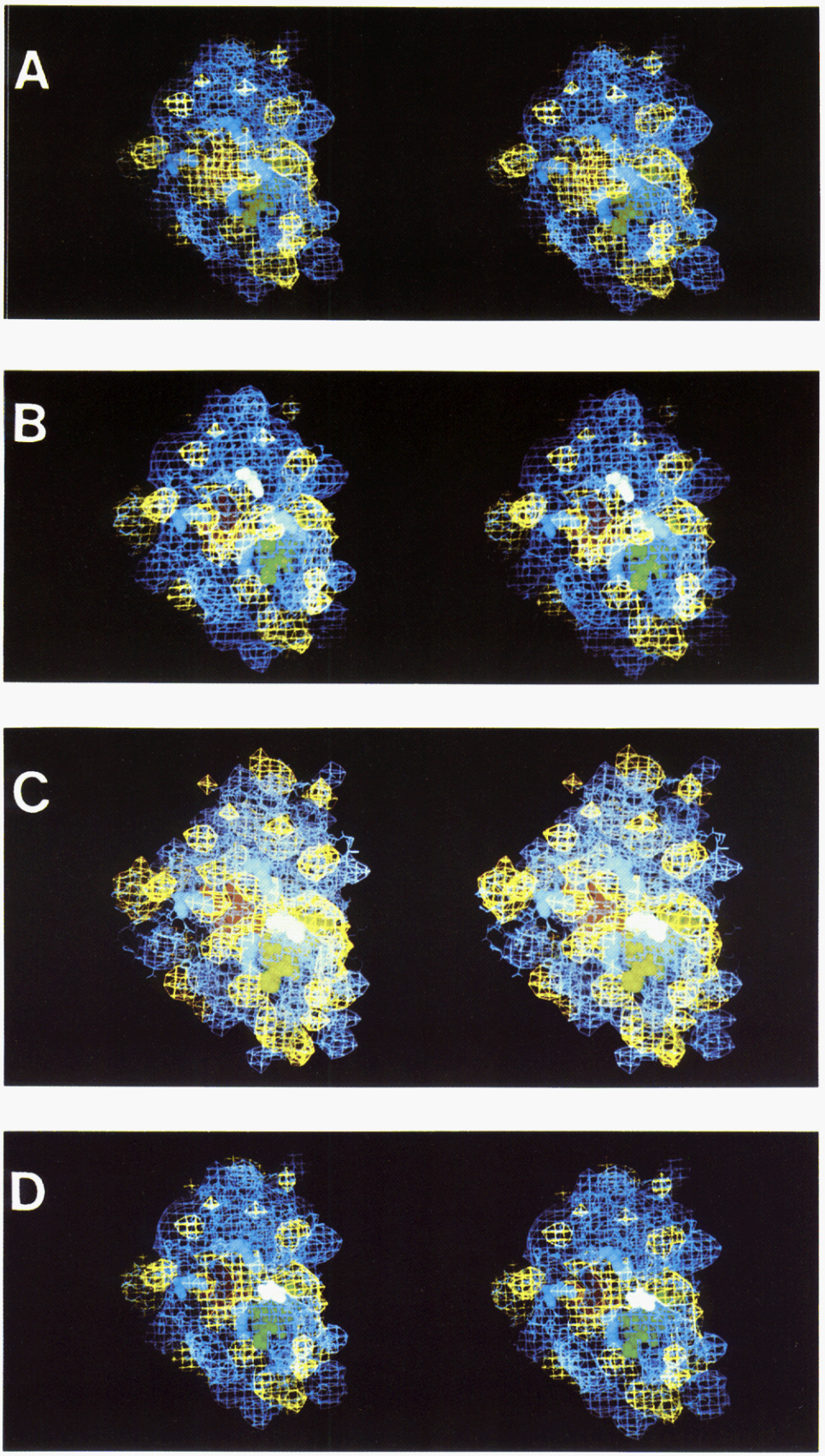

FIGURE 3: Cytochrome P-450$_{cam}$ electrostatic surface calculated at 140 mM ionic strength with a discrete charge library and the linearized Poisson–Boltzmann equation. The backbone and side chains are cyan with modeled cytochrome b_5 electrostatic contacts (Lys 344, Arg 364, Arg 72, Arg 112) represented as CPK surfaces, the K-helix is green and space filled for orientation purposes, and the heme prosthetic group is red. The negative electrostatic surface at an energy level of 3 kT is contoured in blue while the analogous cationic surface is contoured in yellow. Stereoviews of the wild-type and surface mutant cytochrome P-450$_{cam}$ proximal surface showing the cationic patch at the modeled cytochrome b_5 and putidaredoxin interaction site lying directly above the prosthetic heme: (A) wild-type, this proximal view is identical with that calculated for the K392Q mutant; (B) R72Q mutant with the CPK glutamine side chain in white; (C) K344E mutant with the CPK glutamate side chain in white; (D) K344Q mutant with the CPK glutamine side chain in white.

The calculated electrostatic potential field of cytochrome P-450$_{cam}$ provides an interesting theoretical backdrop for the consideration of proposed binding surfaces in the cytochromes P-450. The electrostatic surface is dominated by anionic potential, with the largest continuous cationic patch lying on the proximal surface directly above the thiolate proximal heme ligand and encompassing the previously proposed cytochrome b_5/putidaredoxin binding site (Stayton et al., 1988). This asymmetry is not obvious by simply looking at the distribution of charged residues in the three-dimensional structure. Putidaredoxin has been shown to provide an effector function necessary for the coupling of electron transfer to substrate turnover in addition to its redox role (Lipscomb et al., 1976; Sligar et al., 1974). Intriguing insight into the chemical basis for this activity has been reported recently (Shiro, 1989), where it was suggested that a binding-related reorganization of the electronic structure occurred at either the thiolate–iron axial ligation sphere or at the iron–distal ligand position. It is clear that the results presented here provide an easily visualized structural basis for such effects, since our suggested binding site lies on the proximal surface of nearest approach to the axial thiolate and buried heme prosthetic group. A similar type of effector function has been suggested for adrenodoxin (Tsubaki et al., 1988), and the models discussed here provide an analogous rationale. The cationic patch is connected to the other significant region of positive potential which is localized on the left side of the triangular wedge when looking at the distal surface defined in the standard view of cytochrome P-450$_{cam}$ (Figure 2). The entire distal surface is anionic in character as calculated with discrete charges, possibly resulting in an effective reduction of dimensions that could result in a steering of productive collisions to the more electrostatically favorable proximal surface.

Experimental evidence presented in this paper with surface charge mutants at Lys 344 and Arg 72 correlates well with the calculated effects of basic side chain removal on the proximal patches of cationic electrostatic potential (Figure 3). Recent chemical modification studies with Lys 384 of the eukaryotic cytochrome P-450$_{scc}$ (Tuls et al., 1989; Tsubaki et al., 1989) have implicated the involvement of position 384 in the binding interaction of the analogous Fe_2S_2 iron–sulfur protein adrenodoxin. This residue has been aligned with the K-helix of cytochrome P-450$_{cam}$ (Nelson & Strobel, 1988), which lies directly adjacent to the proximal cationic patch as seen in Figure 3. The aligned primary sequences in this region contain a series of basic amino acids that are conserved in the mitochondrial cytochromes P-450 and represent potential salt bridge contacts with adrenodoxin carboxylates. In addition, conserved hydrophobic residues in this region have been noted which could represent a potential interfacial packing surface. It should be noted that despite these striking similarities adrenodoxin and putidaredoxin are not functionally interchangeable in their respective redox systems (Tsai et al., 1971; Tyson et al., 1972; Geren et al., 1986). Indeed, although the K-helix is located very near the proposed putidaredoxin binding site, it is surrounded by negative electrostatic potential on the cytochrome P-450$_{cam}$ surface, and the lysines modified in cytochrome P-450scc are not present in the aligned P-450$_{cam}$ sequence of Nelson and Strobel (1988). The cross-reactivity of the *Pseudomonas* cytochromes P-450 LIN, CYM, and CAM with the respective redoxin and reductase components has also been reported (Gunsalus et al., 1985). Significant, though lowered, reconstituted activity was observed in some cases, suggesting conserved interaction domains exist to some extent in the bacterial family. Reconstituted cross-reactivity has also been reported with the components of the *Bacillus megaterium* cytochrome P-450 system (Berg et al., 1979). Both adrenodoxin and megaredoxin were cross-reactive in the adrenal and bacterial systems. In addition, the megaredoxin reductase and megaredoxin components were able to reconstitute both P-450$_{11\beta}$ and a microsomal cytochrome P-450 (P-450LM3) activity, suggesting conservation of some surface features may extend to the eukaryotic family.

The second region of cationic potential lying along the side of the triangular wedge defined by cytochrome P-450$_{cam}$ has been suggested as a functional binding region in the eukaryotic cytochromes P-450 on the basis of conserved charge residues in aligned sequences (Nelson & Strobel, 1988). The largest portion of the cationic surface on this side lies directly above cytochrome P-450$_{cam}$ residues 330–340, the region above residues 370–379 of the L-helix, and the C-terminal end of the I-helix. This portion is continuous with the proximal patch lying directly above the heme group as the two are connected by a bridge of positive potential. A second, smaller area of positive potential lies over the β2 area. There is no cationic potential in the region of β3 and β4 as suggested by alignment analysis. In addition, the first region of charge conservation considered by Nelson and Strobel, corresponding to cytochrome P-450$_{cam}$ residues 112–135, is largely associated with negative potential. The calculation of the cytochrome P-450$_{cam}$ electrostatic surface thus supports the hypothesis that the second conserved charge region in the Nelson and Strobel alignment analysis, corresponding to the left side of the triangular wedge in the standard view representation (Figure 2), may represent the binding contact sites for the flavin-linked reductase responsible for providing reducing equivalents to cytochrome P-450 in the liver microsomal systems. To the extent that the cytochrome P-450$_{cam}$ results may be extrapolated to the eukaryotic enzymes, it thus appears that these conserved residues may be arrayed in three-dimensional space to provide complementary electrostatic binding contacts with anionic surfaces of partner proteins. Given the previous competitive binding results with cytochrome b_5 and putidaredoxin (Stayton et al., 1989), an intriguing report of cross-reactivity between the bacterial redoxins and the microsomal cytochrome P-450LM2 (Bernhardt & Gunsalus, 1985) further suggests conservation of some surface features between the bacterial cytochrome P-450$_{cam}$ and some microsomal cytochromes P-450 may exist. It should be noted, however, that the LM2 residue aligned with Lys 314 in cytochrome P-450$_{cam}$ and proposed to be involved in the interaction of the cytochrome with flavoprotein reductase (Bernhardt et al., 1984) is not located in a region of positive potential. Indeed, it is surrounded by negative electrostatic potential, suggesting that direct comparison of eukaryotic cytochrome P-450 structure with cytochrome P-450$_{cam}$ structure should be viewed cautiously. Similarly, separate and distinct binding sites for cytochrome b_5 and P-450 reductase have been observed with cytochrome P-450LM2 (Tamburini & Schenkman, 1987), while cytochrome b_5, cytochrome P-450PB-1, and cytochrome P-450 reductase apparently do not form a ternary complex (Nisimoto & Otsuka-Murakami, 1988), again pointing to cytochrome P-450 specific interactions. The molecular delineation of specific protein–protein interactions across the cytochrome P-450 family will obviously require precise structural information on the eukaryotic systems.

In summary, we have presented experimental evidence for the proposed cytochrome P-450$_{cam}$ binding surface that was previously hypothesized to represent the site of both cytochrome b_5 and putidaredoxin interactions. The calculated

electrostatic surface is entirely consistent with the experimental results and has provided interesting theoretical considerations for binding results reported with eukaryotic cytochromes P-450.

ACKNOWLEDGMENTS

We thank Dr. Thomas Poulos for Figure 2, Tom Loebach for assistance with the DELPHI software, Susan Martinis for the mutant EPR spectra, and Dr. Ling Qin for assistance with the direct electron-transfer experiments.

Registry No. L-Lys, 56-87-1; L-Arg, 74-79-3; L-Gln, 56-85-9; L-Glu, 56-86-0; cytochrome P450, 9035-51-2; cytochrome b_5, 9035-39-6.

REFERENCES

Atkins, W. M., & Sligar, S. G. (1988) *J. Biol. Chem. 263*, 18842–18849.

Beck von Bodman, S., Schuler, M. A., Jollie, D. R., & Sligar, S. G. (1986) *Proc. Natl. Acad. Sci. U.S.A. 83*, 9443–9447.

Berg, A., Ingelman-Sundberg, M., & Gustafsson, J.-A. (1977) *J. Biol. Chem. 254*, 5264–5271.

Bernhardt, R., & Gunsalus, I. C. (1985) in *Cytochrome P-450 Biochemistry, Biophysics, and Induction* (Vereczkey, L., & Magyar, K., Eds.) pp 19–22, Akademia Kiado, Budapest.

Bernhardt, R., Makower, A., Janig, G.-R., & Ruckpaul, K. (1984) *Biochim. Biophys. Acta 785*, 186–190.

Black, S. D., & Coon, M. J. (1987) *Adv. Enzymol. Relat. Areas Mol. Biol. 60*, 35–87.

Brewer, C. B., & Peterson, J. A. (1988) *J. Biol. Chem. 263*, 7791–7798.

Cupp, J. R., & Vickery, L. E. (1988) *J. Biol. Chem. 263*, 17418–17421.

Dailey, H. A., & Strittmatter, P. (1979) *J. Biol. Chem. 254*, 5388–5396.

Ferguson-Miller, S., Brautigan, D. L., & Margoliash, E. (1978) *J. Biol. Chem. 253*, 149–159.

Geren, L. M., & Millett, F. (1981) *J. Biol. Chem. 256*, 4851–4855.

Geren, L. M., O'Brien, P., Stoneheurner, J., & Millett, F., & Peterson, J. A. (1986) *J. Biol. Chem. 261*, 15491–15495.

Gunsalus, I. C., & Wagner, G. C. (1978) *Methods Enzymol. 52*, 166–188.

Gunsalus, I. C., Bhattacharyya, P. K., & Suhara, K. (1985) *Curr. Top. Cell. Regul. 26*, 295–309.

Hackett, C. S., & Strittmatter, P. (1984) *J. Biol. Chem. 259*, 3275–3282.

Hazzard, J. T., McLendon, G., Cusanovich, M. A., Das, G., Sherman, F., & Tollin, G. (1988) *Biochemistry 27*, 4445–4451.

Hildebrant, A. G., & Estabrook, R. W. (1971) *Arch. Biochem. Biophys. 143*, 66–79.

Hintz, M. J., & Peterson, J. A. (1981) *J. Biol. Chem. 256*, 6721–6728.

Hintz, M. J., Mock, D. M., Peterson, L. L., Tuttle, K., & Peterson, J. A. (1982) *J. Biol. Chem. 257*, 14324–14332.

Kang, C. H., Brautigan, D. L., Osheroff, N., & Margoliash, E. (1978) *J. Biol. Chem. 253*, 6502–6510.

Koga, H., Rauchfuss, B., & Gunsalus, I. C. (1985) *Biochem. Biophys. Res. Commun. 130*, 412–417.

Koppenol, W. H., & Margoliash, E. (1982) *J. Biol. Chem. 257*, 4426–4437.

Lambeth, J. D., Geren, L. M., & Millett, F. (1984) *J. Biol. Chem. 259*, 10025–10029.

Lipscomb, J. D., Sligar, S. G., Namtvedt, M. J., & Gunsalus, I. C. (1976) *J. Biol. Chem. 251*, 1116–1124.

Livingston, D. J., McLachlan, S. J., La Mar, G. N., & Brown, W. D. (1985) *J. Biol. Chem. 260*, 15699–15707.

Matthews, F. S., Levine, M., & Argos, P. (1972) *J. Mol. Biol. 64*, 449–464.

Mauk, M. R., & Mauk, A. G. (1972) *Biochemistry 21*, 4730–4734.

Morgan, E. T., & Coon, M. J. (1984) *Drug Metab. Dispos. 12*, 358–364.

Nadler, S. G., & Strobel, H. W. (1988) *Arch. Biochem. Biophys. 261*, 418–429.

Nelson, D. R., & Strobel, H. W. (1988) *J. Biol. Chem. 263*, 6038–6050.

Nelson, D. R., & Strobel, H. W. (1989) *Biochemistry 28*, 656–660.

Ng, S., Smith, M. B., Smith, H. T., & Millett, F. (1977) *J. Biol. Chem. 16*, 4975–4978.

Nisimoto, Y., & Otsuka-Murakami, H. (1988) *Biochemistry 27*, 5869–5876.

Northrup, S. H., Boles, J. O., & Reynolds, J. C. L. (1988) *Science 241*, 67–70.

Pederson, T. C., Austin, R. H., & Gunsalus, I. C. (1977) in *Microsomes & Drug Oxidations* (Ullrich, V., Ed.) pp 275–283, Pergamon Press, Oxford, U.K.

Pompon, D., & Coon, M. J. (1984) *J. Biol. Chem. 259*, 15377–15385.

Poulos, T. L., & Mauk, A. G. (1983) *J. Biol. Chem. 258*, 7369–7373.

Poulos, T. L., & Howard, A. J. (1987) *Biochemistry 26*, 8165–8174.

Poulos, T. L., Finzel, B. C., Gunsalus, I. C., Wagner, G. C., & Kraut, J. (1985) *J. Biol. Chem. 260*, 16122–16130.

Poulos, T. L., Finzel, B. C., & Howard, A. J. (1986) *Biochemistry 25*, 5314–5322.

Poulos, T. L., Finzel, B. C., & Howard, A. J. (1987) *J. Mol. Biol. 195*, 687–700.

Rodgers, K. K., Pochapsky, T. C., & Sligar, S. G. (1988) *Science 240*, 1657–1659.

Salemme, F. R. (1976) *J. Mol. Biol. 102*, 563–568.

Shiro, Y., Iizuka, T., Makino, R., Ishimura, Y., & Morishima, I. (1989) *J. Am. Chem. Soc. 111*, 7707–7711.

Stayton, P. S., Fisher, M. T., & Sligar, S. G. (1988) *J. Biol. Chem. 263*, 13544–13548.

Stayton, P. S., Poulos, T. L., & Sligar, S. G. (1989) *Biochemistry 28*, 8201–8205.

Tamburini, P. P., & Schenkman, J. B. (1987) *Proc. Natl. Acad. Sci. U.S.A. 84*, 11–15.

Tamburini, P. P., White, R. E., & Schenkman, J. B. (1985) *J. Biol. Chem. 260*, 4007–4015.

Taylor, J. W., Ott, J., & Eckstein, F. (1985) *Nucleic Acids Res. 13*, 8764–8785.

Tsai, R. L., Gunsalus, I. C., & Dus, K. (1971) *Biochem. Biophys. Res. Commun. 45*, 1300–1306.

Tsubaki, M., Hiwatashi, A., Ichikawa, Y., Fujimoto, Y., Ikekawa, N., & Hori, H. (1988) *Biochemistry 27*, 4856–4862.

Tsubaki, M., Iwamoto, Y., Hiwatashi, A., & Ichikawa, Y. (1989) *Biochemistry 28*, 6899–6907.

Tuls, J., Geren, L., & Millett, F. (1989) *J. Biol. Chem. 264*, 16421–16425.

Tyson, C. A., Lipscomb, J. D., & Gunsalus, I. C. (1972) *J. Biol. Chem. 262*, 10020–10025.

Unger, B. P., Gunsalus, I. C., & Sligar, S. G. (1986) *J. Biol. Chem. 261*, 1158–1163.

Warshel, A., & Russell, S. T. (1984) *Q. Rev. Biophys. 17*, 283–422.

Wendoloski, J. J., Matthew, J. B., Weber, P. C., & Salemme, F. R. (1987) *Science 238*, 794–797.